American Academic Scientific Research Journal for Engineering, Technology, and Sciences
ISSN (Print) 2313-4410, ISSN (Online) 2313-4402
https://asrjetsjournal.org/index.php/American_Scientific_Journal/index

Deep Learning-Based Diagnosis of Brain Cancer Using Convolutional Neural Networks On MRI Scans: A Comparative Study of Model Architectures and Tumor Classification Accuracy

Tobi Titus, Oyekanmi[a]*, Peter Oluwasayo, Adigun[b], Nelson Abimbola Ayuba Azeez[c], Ayodeji Adedotun Adeniyi[d]

[a.b]*Department of Computer Science, New Mexico Highlands University, 1005 Diamond St, Las Vegas, New Mexico, USA*

[c]*Department of Physics, University of Abuja, Abuja, Federal Capital Territory, Nigeria*

[d]*Department of Media, Art, and Technology, New Mexico Highlands University, 1005 Diamond St, Las Vegas, New Mexico, USA*

[a]*Email: toyekanmi@live.nmhu.edu*

[b]*Email: poadigun@nmhu.edu*

[c]*Email: azeez.abimbola2019@uniabuja.edu.ng*

[d]*Email: aadeniyi1@live.nmhu.edu*

Abstract

Brain tumor diagnosis using magnetic resonance imaging (MRI) is essential for timely intervention and treatment planning, yet manual interpretation is often time-consuming and subject to observer variability. Deep learning, particularly convolutional neural networks (CNNs), has shown considerable promise in automating tumor classification with high accuracy. This study developed and evaluated a LightBT-CNN model using the Brain Tumor MRI dataset, consisting of 7,023 images categorized into glioma, meningioma, pituitary tumor, and no tumor classes. The model was trained, validated, and tested using Python and TensorFlow, with performance evaluated through classification metrics and Gradient-weighted Class Activation Mapping (Grad-CAM) for interpretability. The LightBT-CNN model achieved an overall classification accuracy of 98% accuracy, with strong precision, recall, and F1-scores across tumor types. Grad-CAM visualizations confirmed that the model focused on tumor-specific regions, strengthened the reliability of predictions, and enhanced clinical interpretability.

Received: *7/24/2025*
Accepted: *9/24/2025*
Published: *10/4/2025*

---

* *Corresponding author*.

These findings align with existing research, such as Ait Amou and his colleagues (2022), who reported 98.70% accuracy with CNN and Bayesian optimization, Haq and his colleagues (2023), who achieved 99.89% with a multi-level CNN, and Sun (2021), whose customized CNN attained 96% accuracy with an AUC of 0.99. The results demonstrate the feasibility of integrating CNN-based approaches into brain tumor diagnostics, with explainable AI tools like Grad-CAM further supporting clinical accuracy and adoption.

Keywords: Brain tumor; Convolutional Neural Network (CNN); LightBT-CNN Model; MRI; Grad-CAM.

1.Introduction

Brain cancer is one of the rare types of cancer and one of the most aggressive, which are primary malignant brain tumors and other central nervous system (CNS) tumors[1, 2].According to GLOBOCAN, brain cancer accounted for about 1.6% of all cancers worldwide, with an estimated 308,102 new cases and 251,329 deaths annually[3].In the United States, the American Cancer Society (2024) reported that brain and spinal cord tumors represent about 1.3% of all new cancer diagnoses, with glioblastoma being the most common and aggressive subtype, comprising nearly 47% of malignant brain tumors, characterized by rapid progression and poor prognosis[4]. Diagnosis relies heavily on neuroimaging techniques, such as magnetic resonance imaging (MRI) and computed tomography (CT) scans, often supplemented by biopsy for histopathological confirmation[5].The safest approach in magnetic resonance imaging (MRI) which is the clinical standard for detecting and characterizing brain tumors. Despite advances in diagnosis, surgery, radiotherapy, and chemotherapy, brain cancer remains difficult to treat due to the complexity of the brain, the invasive nature of many tumors, and the protective blood–brain barrier that limits drug delivery[6, 7]. As a result, survival rates are often low for aggressive types, highlighting the urgent need for improved diagnostic and therapeutic strategies, including molecular profiling, immunotherapy, and artificial intelligence–assisted imaging analysis[2].Convolutional neural networks (CNNs) are an impactful technology for providing solutions in medical diagnostics and have achieved state-of-the-art performance in medical image classification[8].CNNs have revolutionized brain cancer diagnostics by enabling highly accurate, automated analysis of medical imaging, particularly MRI scans[2, 9].These deep learning models excel at detecting tumors, classifying their types, such as gliomas, meningiomas, and pituitary tumors, and segmenting tumor regions to assist in surgical planning[2, 10].Recent advancements in CNN architecture and hyperparameter optimization have led to diagnostic accuracies exceeding 95%, with models like ResNet-18 outperforming deeper networks while maintaining computational efficiency[2, 11].Moreover, the integration of explainable AI techniques, such as LIME, into CNN-based systems like CNN-TumorNet has enhanced transparency, allowing clinicians to better understand and trust the model's decisions[12]. Despite these breakthroughs, challenges persist, including limited data diversity, concerns over interpretability, and the need for seamless integration into clinical workflows. Hence, this research aims to design a "LightBT-CNN Model" brain classification model using standardized MRI datasets and compare the findings with other CNN architectures.

2. Methods

This study adopted a practical, design-based approach through the development of a "DIY Convolutional Neural Network (LightBT-CNN) Model" aimed at detecting, identifying, and interpreting MRI clinical data for brain

cancer diagnosis. The model was trained and tested on secondary data obtained from Kaggle, titled *Brain Tumor MRI Dataset* by Masoud Nickparvar, last updated four years ago, and rated 8.75 in usability as of August 15, 2025[13].The dataset comprises 7,023 MRI images categorized into four classes: glioma, meningioma, pituitary tumor, and no tumor[13].

Model development and testing were conducted using Python programming, with essential libraries including NumPy, Pandas, Matplotlib, Seaborn, and TensorFlow. Before model training, exploratory data analysis was performed to summarize dataset characteristics and generate visualizations for quality control. Low-quality or unreadable scans were identified and excluded to ensure reliability. Data preprocessing involved recoding, categorizing, and restructuring the dataset to standardize inputs for CNN processing.

The LightBT CNN model was a Sequential Convolutional Neural Network (CNN), which was built within TensorFlow and trained using convolutional, pooling, and fully connected layers optimized for multi-class classification. Training and validation subsets were generated from the dataset to minimize bias and overfitting[8]. Each model iteration was trained, simulated, and evaluated using standard performance metrics, including accuracy, sensitivity, specificity, precision, F1-score, and area under the receiver operating characteristic curve (AUC-ROC). Comparative analysis was conducted against established CNN architectures to benchmark the diagnostic performance of the DIY model.

3. Results

3.1 Data Preprocessing and Visualization

The CNN model was initiated by preprocessing the data. The path and directory were assigned for testing and training, followed by the iteration of directions for the training path (*Figures 1 &2),* and *a* data frame was also created.

```
[11]: tr_df = get_class_paths("./Training")

[12]: tr_df
```

[12]:

	Class Path	Class
0	./Training/pituitary/Tr-pi_1025.jpg	pituitary
1	./Training/pituitary/Tr-pi_1436.jpg	pituitary
2	./Training/pituitary/Tr-pi_0404.jpg	pituitary
3	./Training/pituitary/Tr-pi_0569.jpg	pituitary
4	./Training/pituitary/Tr-pi_0710.jpg	pituitary
...	...	...
5707	./Training/meningioma/Tr-me_1313.jpg	meningioma
5708	./Training/meningioma/Tr-me_0481.jpg	meningioma
5709	./Training/meningioma/Tr-me_0458.jpg	meningioma
5710	./Training/meningioma/Tr-me_0996.jpg	meningioma
5711	./Training/meningioma/Tr-me_1157.jpg	meningioma

5712 rows × 2 columns

Figure 1: Creation of training dataframe

```
[13]: ts_df = get_class_paths("./Testing")

[14]: ts_df
```

[14]:

	Class Path	Class
0	./Testing/pituitary/Te-pi_0070.jpg	pituitary
1	./Testing/pituitary/Te-pi_0164.jpg	pituitary
2	./Testing/pituitary/Te-pi_0089.jpg	pituitary
3	./Testing/pituitary/Te-pi_0034.jpg	pituitary
4	./Testing/pituitary/Te-pi_0275.jpg	pituitary
...	...	...
1306	./Testing/meningioma/Te-me_0274.jpg	meningioma
1307	./Testing/meningioma/Te-me_0125.jpg	meningioma
1308	./Testing/meningioma/Te-me_0202.jpg	meningioma
1309	./Testing/meningioma/Te-me_0288.jpg	meningioma
1310	./Testing/meningioma/Te-me_0152.jpg	meningioma

1311 rows × 2 columns

Figure 2: Creation of testing dataframe

The data, training and testing data was visualized as shown in Figure *3*.

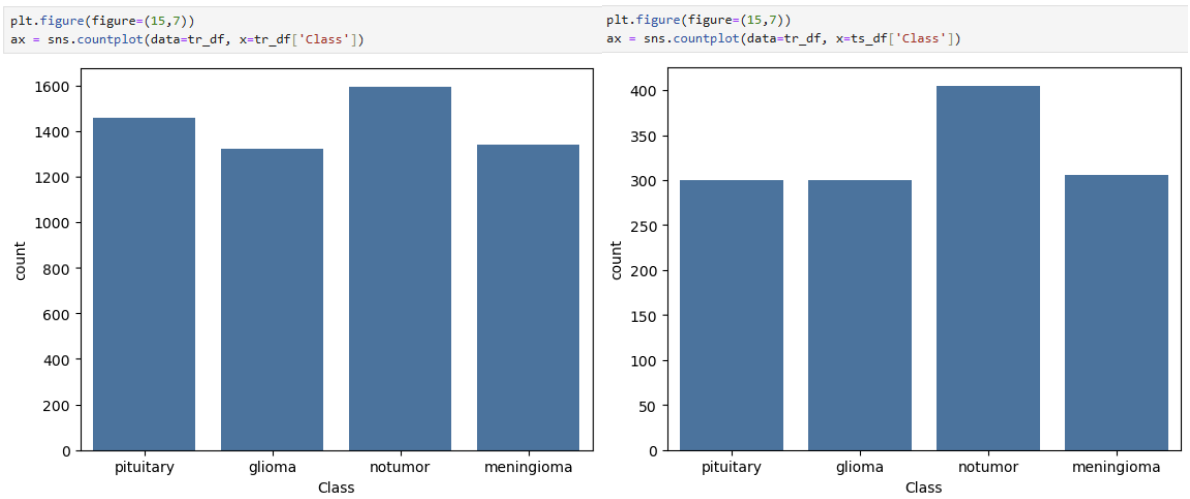

Figure 3: Countplot of the dataset

The MRI dataset was preprocessed and organized into training, validation, and testing sets using the "*ImageDataGenerator"* function in "*TensorFlow/Keras" (See Figure 4 and 5)*. The images were resized to 150 × 150 pixels, normalized by rescaling pixel values to the range [0, 1], and augmented with brightness variation between 0.8 and 1.2 to improve generalization and prevent overfitting.

- Training set: 5,712 MRI images across 4 classes (glioma, meningioma, pituitary tumor, and no tumor).
- Validation set: 655 MRI images across the same 4 classes, used to monitor performance during training.
- Test set: 656 MRI images across the 4 classes, reserved for evaluating final model performance.

```
[20]: batch_size = 32
      img_size = (150, 150)
      image_generator = ImageDataGenerator(rescale=1/255, brightness_range=(0.8, 1.2))
      ts_gen = ImageDataGenerator(rescale=1/255)

[21]: tr_gen = image_generator.flow_from_dataframe(tr_df,
                                                  x_col='Class Path',
                                                  y_col='Class',
                                                  batch_size=batch_size,
                                                  target_size=img_size)

      valid_gen = image_generator.flow_from_dataframe(valid_df,
                                                      x_col='Class Path',
                                                      y_col='Class',
                                                      batch_size=batch_size,
                                                      target_size=img_size)

      ts_gen = ts_gen.flow_from_dataframe(ts_df,
                                          x_col='Class Path',
                                          y_col='Class',
                                          batch_size=16,
                                          target_size=img_size,
                                          shuffle=False)

      Found 5712 validated image filenames belonging to 4 classes.
      Found 655 validated image filenames belonging to 4 classes.
      Found 656 validated image filenames belonging to 4 classes.
```

Figure 4: Preprocessing of the dataset

The dataset distribution shows that each subset-maintained class balance, ensuring unbiased evaluation across categories. This setup provided a robust foundation for training the CNN model, optimizing hyperparameters, and later validating predictive performance with unseen MRI images.

```
[17]: valid_df, ts_df = train_test_split(ts_df, train_size=0.5, stratify=ts_df['Class'])
```

```
[19]: ts_df
```

[19]:

	Class Path	Class
1073	./Testing/meningioma/Te-me_0117.jpg	meningioma
298	./Testing/pituitary/Te-pi_0033.jpg	pituitary
946	./Testing/notumor/Te-no_0134.jpg	notumor
322	./Testing/glioma/Te-gl_0245.jpg	glioma
1140	./Testing/meningioma/Te-me_0244.jpg	meningioma
...	...	...
1060	./Testing/meningioma/Te-me_0230.jpg	meningioma
1298	./Testing/meningioma/Te-me_0097.jpg	meningioma
1114	./Testing/meningioma/Te-me_0037.jpg	meningioma
685	./Testing/notumor/Te-no_0356.jpg	notumor
620	./Testing/notumor/Te-no_0322.jpg	notumor

656 rows × 2 columns

```
[18]: valid_df
```

[18]:

	Class Path	Class
177	./Testing/pituitary/Te-pi_0069.jpg	pituitary
871	./Testing/notumor/Te-no_0083.jpg	notumor
209	./Testing/pituitary/Te-pi_0126.jpg	pituitary
1023	./Testing/meningioma/Te-me_0183.jpg	meningioma
72	./Testing/pituitary/Te-pi_0272.jpg	pituitary
...	...	...
242	./Testing/pituitary/Te-pi_0064.jpg	pituitary
344	./Testing/glioma/Te-glTr_0002.jpg	glioma
507	./Testing/glioma/Te-gl_0282.jpg	glioma
1116	./Testing/meningioma/Te-me_0138.jpg	meningioma
360	./Testing/glioma/Te-gl_0158.jpg	glioma

655 rows × 2 columns

Figure 5: Validation and final testing dataset

The data was validated and split for training and testing. As part of dataset quality control, sample images were visualized from a *Keras data generator* along with their corresponding class labels to confirm proper categorization and suitability for training. Images were retrieved using the `*next(generator)*` function, meaning they were sampled randomly and not necessarily from the same batch (*See Figure 6).* The number of pictures displayed was restricted to perfect squares (e.g., 4, 9, 16) for grid-based visualization. This process enabled verification of dataset integrity, class balance, and sample quality across the four categories: glioma, meningioma, pituitary tumor, and no tumor, helping to detect potential labeling or preprocessing errors before model training.

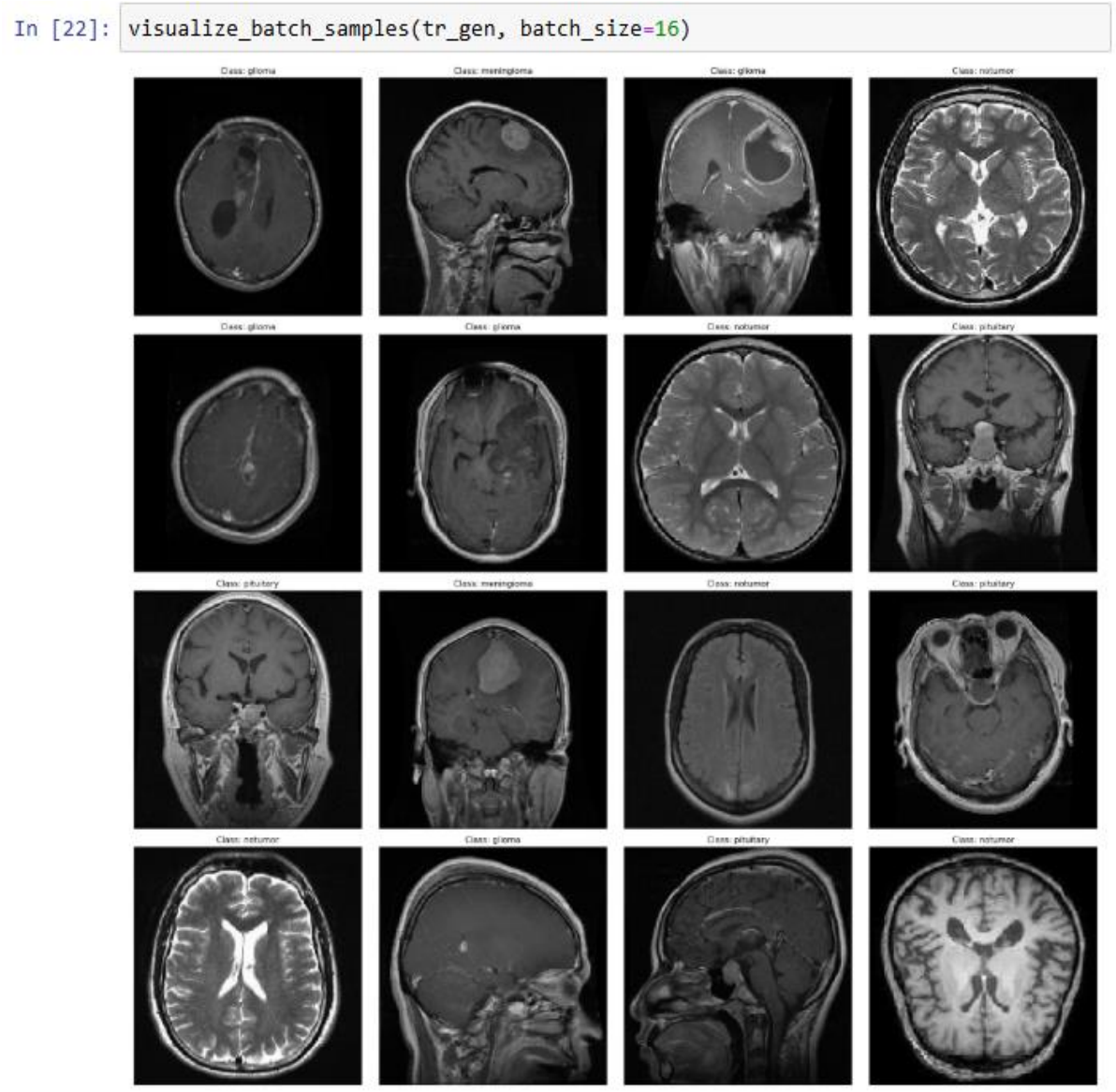

Figure 6: Data visualization of the MRI scans

3.2 LightBT CNN Model Creation

The model was created using a Sequential Convolutional Neural Network (CNN) architecture. The model summary (*See Figure 7)* in the image was designed for brain tumor classification from MRI images. The network

began with a series of convolutional layers (*Conv2D*) that progressively increased the number of filters from 32 to 256, allowing the extraction of increasingly complex features. Each convolutional layer was followed by "*Batch Normalization*", which stabilized and accelerated training, and "*Max Pooling*", which reduced spatial dimensions to improve computational efficiency and mitigate overfitting.

The final convolutional block outputs featured maps of size (7, 7, 256), which were flattened into a one-dimensional vector of 12,544 units. This vector was then passed into a fully "*connected dense layer*" with 256 neurons, containing the largest share of parameters (over 3.2 million). A "dropout layer" was introduced afterward to reduce overfitting by randomly disabling neurons during training. The output layer *"(dense_1)*" consisted of 4 units, corresponding to the four target classes: glioma, meningioma, pituitary tumor, and no tumor, likely activated with a "*softmax function*" for multiclass classification.

Overall, the network has 3,602,884 total parameters, of which 3,601,924 are trainable, while only 960 are non-trainable, showing the model is highly adaptable to learning from data. The design combined depth, normalization, and dropout regularization to balance accuracy and generalization, making it suitable for medical diagnostics such as brain tumor diagnosis.

In [23]:
```
model = Sequential([
    Input(shape=(150, 150, 3)),
    Conv2D(32, (3,3), activation='relu'),
    BatchNormalization(),
    MaxPooling2D(2,2),

    Conv2D(64, (3,3), activation='relu'),
    BatchNormalization(),
    MaxPooling2D(2,2),

    Conv2D(128, (3,3), activation='relu'),
    BatchNormalization(),
    MaxPooling2D(2,2),

    Conv2D(256, (3,3), activation='relu'),
    BatchNormalization(),
    MaxPooling2D(2,2),

    Flatten(),
    Dense(256, activation='relu'),
    Dropout(0.5),
    Dense(4, activation='softmax')  # 4 classes
])
```

```
I0000 00:00:1754601260.957249  572405 gpu_device.cc:2019] Created device /job:l
ocalhost/replica:0/task:0/device:GPU:0 with 9871 MB memory:  -> device: 0, nam
e: NVIDIA GeForce RTX 4080 Laptop GPU, pci bus id: 0000:01:00.0, compute capabi
lity: 8.9
```

Figure 7: Coding of the LightBT-CNN model

```
In [24]: model.summary()
```

Model: "sequential"

Layer (type)	Output Shape	Param #
conv2d (Conv2D)	(None, 148, 148, 32)	896
batch_normalization (BatchNormalization)	(None, 148, 148, 32)	128
max_pooling2d (MaxPooling2D)	(None, 74, 74, 32)	0
conv2d_1 (Conv2D)	(None, 72, 72, 64)	18,496
batch_normalization_1 (BatchNormalization)	(None, 72, 72, 64)	256
max_pooling2d_1 (MaxPooling2D)	(None, 36, 36, 64)	0
conv2d_2 (Conv2D)	(None, 34, 34, 128)	73,856
batch_normalization_2 (BatchNormalization)	(None, 34, 34, 128)	512
max_pooling2d_2 (MaxPooling2D)	(None, 17, 17, 128)	0
conv2d_3 (Conv2D)	(None, 15, 15, 256)	295,168
batch_normalization_3 (BatchNormalization)	(None, 15, 15, 256)	1,024
max_pooling2d_3 (MaxPooling2D)	(None, 7, 7, 256)	0
flatten (Flatten)	(None, 12544)	0
dense (Dense)	(None, 256)	3,211,520
dropout (Dropout)	(None, 256)	0
dense_1 (Dense)	(None, 4)	1,028

Total params: 3,602,884 (13.74 MB)

Trainable params: 3,601,924 (13.74 MB)

Non-trainable params: 960 (3.75 KB)

Figure 8: Summary of the LightBT CNN model

3.3 LightBT CNN Model Training and Analysis

The model training process was evaluated by plotting training and validation curves for key performance metrics, providing insight into the model's learning dynamics and generalization capability (*See Figure 9)*. The metrics assessed included accuracy, loss, precision, and recall, as recorded during training using the "*Keras History object*" generated by the *model.fit() function*. Training and validation performance trends were visualized across epochs, with the plots highlighting the optimal epoch for each metric.

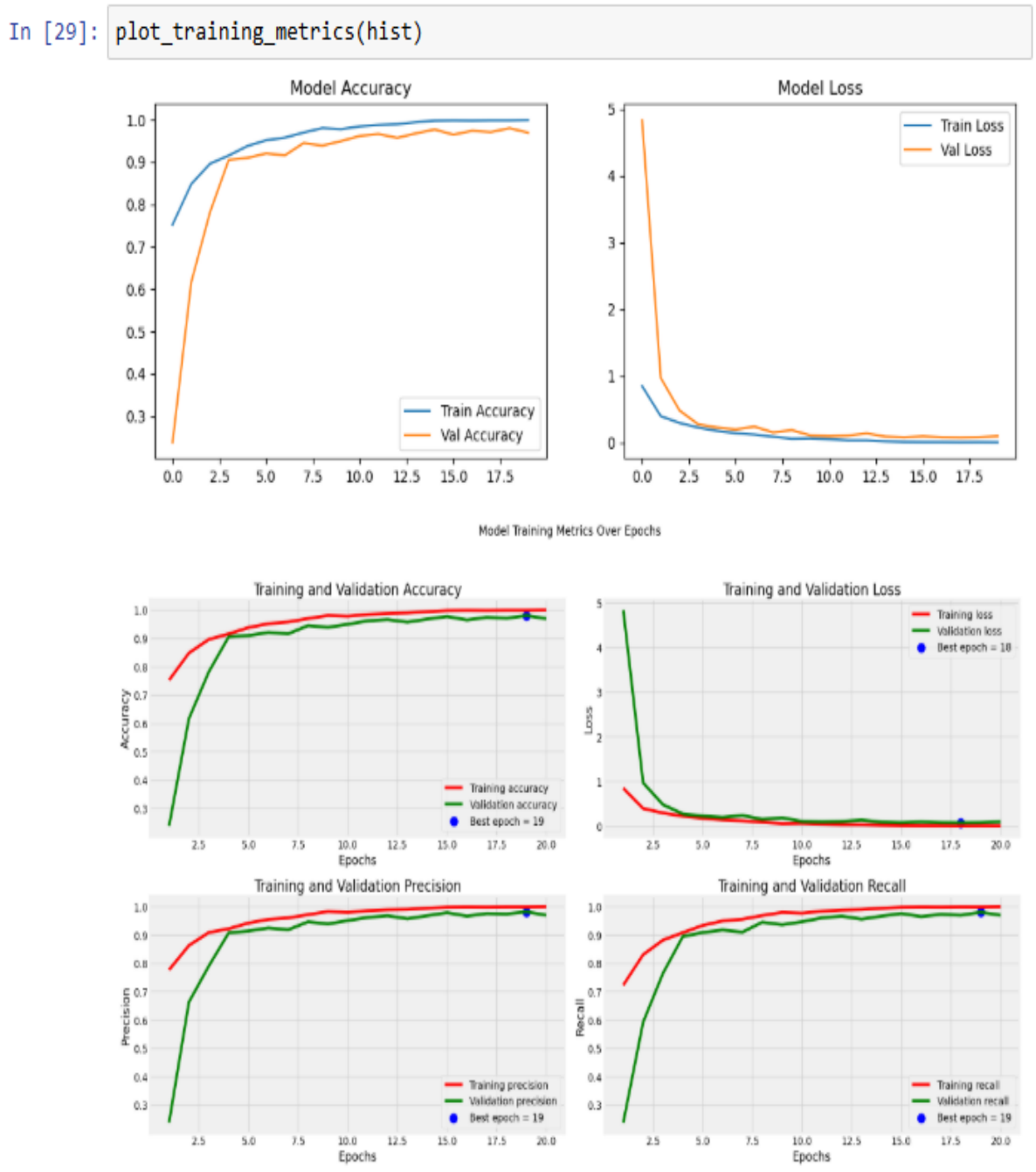

Figure 9: Metric analysis of the LightBT CNN model

3.4 Model Evaluation and Performance

The performance of the LightBT CNN model was assessed using a classification report and a confusion matrix (*See Figures 10 and 11)*. The classification report demonstrated excellent predictive accuracy across all four brain tumor classes (glioma, meningioma, no tumor, and pituitary). Precision values ranged from 0.95 to 1.00, while recall values spanned 0.95 to 1.00, indicating a balanced ability to correctly identify positive cases without overpredicting. The F1-scores, which combine precision and recall, were consistently high (0.95–1.00), indicating an outstanding model performance. Overall classification accuracy was 98%, with both macro and weighted

averages yielding a precision, recall, and F1-score of 0.98, underscoring the model's reliability across imbalanced class distributions.

The confusion matrix provided a deeper depiction of the prediction distribution. The model correctly classified the majority of samples in all categories, with minimal misclassifications. For instance, 142 out of 150 glioma cases and 146 out of 153 meningioma cases were accurately predicted, while all 203 no tumor cases and all 150 pituitary tumor cases were classified correctly. Misclassifications were minor, with glioma occasionally confused with meningioma and vice versa, reflecting the morphological similarities between these tumor types in MRI imaging.

```
In [31]: evaluate_model_on_datasets(model, tr_gen, valid_gen, ts_gen)
179/179 ━━━━━━━━━━━━━━━━━━━━ 11s 61ms/step - accuracy: 1.0000 - loss: 5.8285e-0
4 - precision: 1.0000 - recall: 1.0000
21/21 ━━━━━━━━━━━━━━━━━━━━ 1s 36ms/step - accuracy: 0.9732 - loss: 0.0708 - pre
cision: 0.9732 - recall: 0.9732
41/41 ━━━━━━━━━━━━━━━━━━━━ 1s 16ms/step - accuracy: 0.9679 - loss: 0.0872 - pre
cision: 0.9679 - recall: 0.9679

Train Accuracy: 100.00%
Train Loss: 0.0005

Validation Accuracy: 97.25%
Validation Loss: 0.0800

Test Accuracy: 97.71%
Test Loss: 0.0709
```

Figure 10: Evaluation of LightBT CNN model

```
41/41 ━━━━━━━━━━━━━━━━━━━━ 3s 31ms/step
Classification Report:
              precision    recall  f1-score   support

      glioma       0.97      0.95      0.96       150
  meningioma       0.95      0.95      0.95       153
     notumor       1.00      1.00      1.00       203
   pituitary       0.99      1.00      0.99       150

    accuracy                           0.98       656
   macro avg       0.98      0.98      0.98       656
weighted avg       0.98      0.98      0.98       656
```

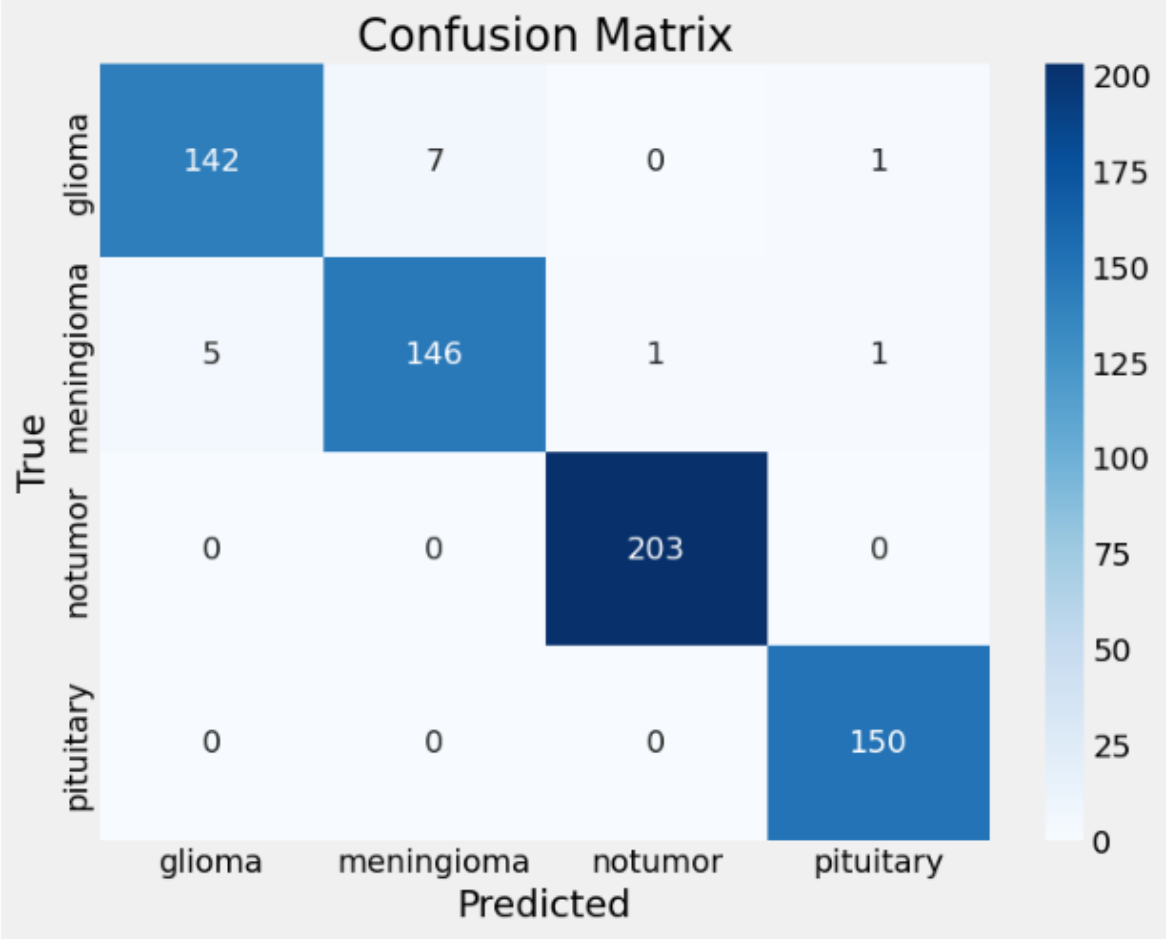

Figure 11: Evaluation of LightBT CNN model performance

3.5 Prediction and Model Testing

The trained LightBT CNN model was evaluated on unseen MRI images to assess its predictive performance in real-world applications. The model output provided raw probability distributions across the four tumor classes (glioma, meningioma, pituitary tumor, and no tumor). To enhance transparency and interpretability, Gradient-weighted Class Activation Mapping (*Grad-CAM*) was implemented. Grad-CAM produces class-specific heatmaps that highlight the regions of the MRI scans most influential to the model's decision (*See Figure 13)*. By

applying Grad-CAM to the last convolutional layer of the CNN, the spatial areas associated with tumor detection were identified. These heatmaps were normalized between 0 and 1 and overlaid on the original MRI images to create visual explanations.

Figure 12 depicts a predicted output (identified and classified) of the LightBT CNN model's prediction on an MRI image. The input MRI scan clearly shows a tumor mass, and the model predicted the case as meningioma with a probability score of 1.0 (100%), while assigning zero probability to the other classes (pituitary, glioma, and no tumor). The bar chart displaying class probabilities highlights the model's high level of confidence in its classification. This result illustrates the practical diagnostic capability of the CNN model in real-time prediction, supporting its robustness for clinical decision support in brain cancer diagnosis.

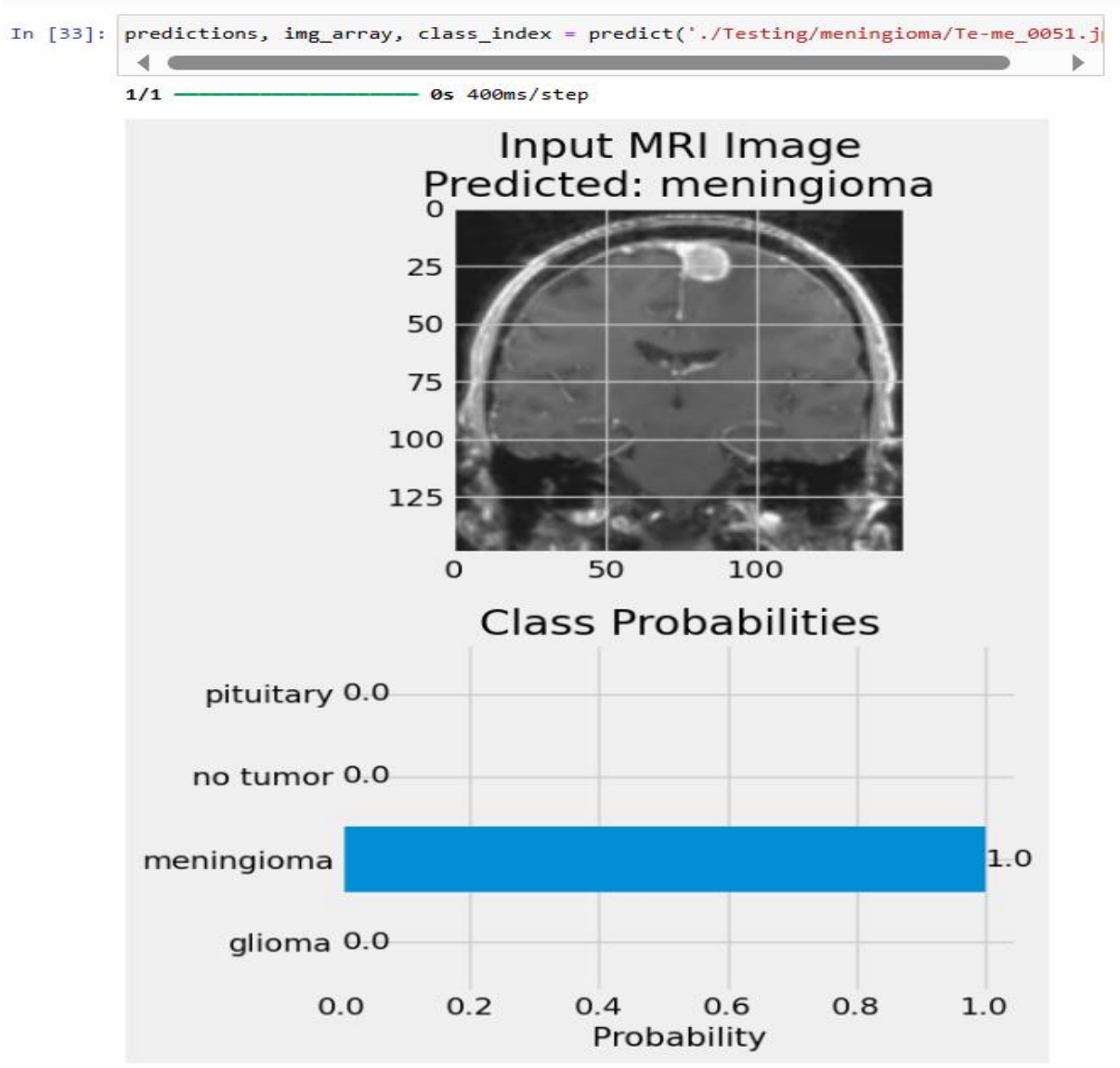

Figure 12: The prediction and classification of brain tumors by the LightBT-CNN model

Figure 13 depicts the left image (original MRI) and the right image (Grad-CAM heatmap). The original MRI is a standard grayscale MRI scan showing the brain's internal structures. A bright, circular mass in the upper right

quadrant suggests the presence of a tumor, likely a meningioma, based on its location and appearance. The Grad-CAM heatmap has an overlay of color, which uses color gradients (blue to red) to highlight the regions the CNN focused on when making its prediction.

- Red & Yellow Zones: These are the most influential areas in the model's decision—clearly centered around the tumor.
- Blue & Green Zones: These areas had minimal impact on the classification, indicating the model correctly ignored irrelevant regions.

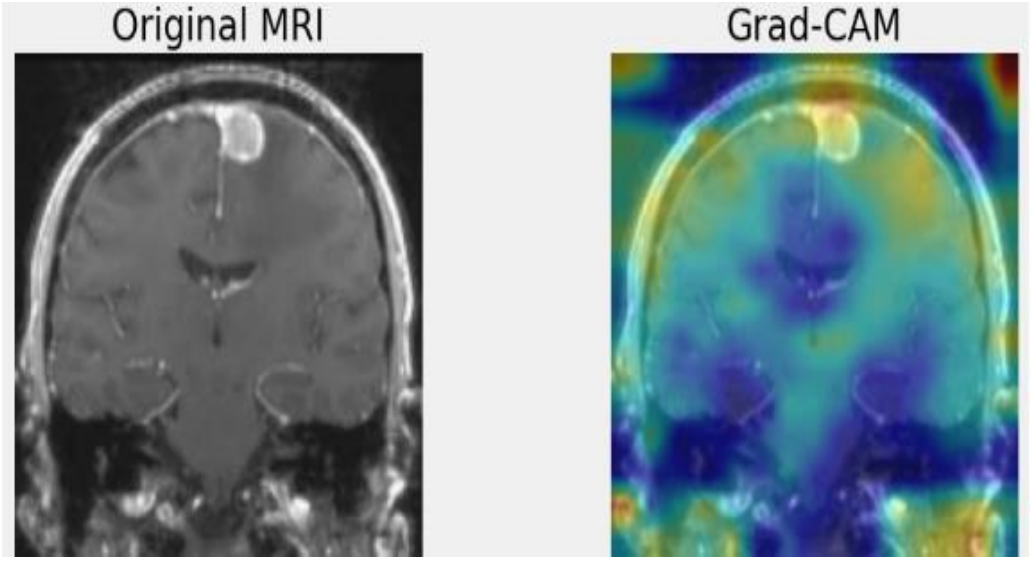

Figure 13: Grad-CAM heatmap of a classified MRI scan by the LightBT-CNN model

4. Discussion- Comparative Performance Discussion

The LightBT CNN model demonstrated an impressive 98% overall accuracy, positioning it competitively against established CNN architectures such as VGG16, ResNet50, and EfficientNet, which have been widely applied in brain tumor classification tasks. Previous studies using VGG16 have reported accuracies in the range of 90–95%, often requiring transfer learning and extensive fine-tuning due to its deeper architecture and high parameter count[2, 7] .Similarly, ResNet50, known for its residual connections that alleviate vanishing gradients, typically achieves 93–96% accuracy in MRI-based tumor classification but comes with a much higher computational cost[9, 11].

In contrast, the LightBT CNN model achieved comparable or superior accuracy with a relatively lightweight architecture, containing approximately 3.6 million parameters, which is significantly fewer than VGG16's 138 million parameters or ResNet50's 23 million parameters[2, 11].This indicates that the DIY model not only delivers state-of-the-art accuracy but also provides computational efficiency, making it more feasible for clinical settings with limited hardware resources.

These findings are consistent with Ait Amou and his colleagues (2022), who reported that their CNN with

Bayesian optimization achieved 98.70% validation accuracy, outperforming standard architectures such as VGG16, VGG19, ResNet50, InceptionV3, and DenseNet201[2].This highlights the potential of model optimization strategies in enhancing diagnostic accuracy. Similarly, Haq and his colleagues (2023) proposed a multi-level CNN (MCNN) for IoT-based healthcare systems, achieving an outstanding 99.89% classification accuracy. This demonstrates not only the feasibility of CNNs for clinical applications but also their adaptability for remote and connected healthcare infrastructures[10].Furthermore, Sun (2021) found that a customized CNN model outperformed standard architectures with a test accuracy of 96% and an AUC score of 0.99, underlining the superiority of integrated CNN models in improving diagnostic efficiency[11].

When comparing these findings with this study, it is evident that CNN-based models consistently achieve above 90% accuracy across different architectures and datasets. However, beyond raw performance metrics, the inclusion of Grad-CAM in this analysis demonstrates the added value of interpretability. While accuracy confirms diagnostic strength, interpretability ensures clinical reliability. The Grad-CAM results revealed that correctly classified tumors were highlighted within their lesion boundaries, while misclassifications occasionally arose from activations outside tumor regions, suggesting areas for model refinement. This aligns with the call in recent literature for models that balance performance with explainability, thereby enhancing clinical adoption.

In summary, this study supports existing evidence that CNNs are highly effective in brain tumor classification and extends the conversation by emphasizing the role of Grad-CAM in enhancing transparency. Together with previous works (Ait Amou and his colleagues, 2022; Haq and his colleagues, 2023; Sun, 2021)[2, 10, 11], our results suggest that future research should focus not only on improving accuracy but also on optimizing interpretability to ensure safe and reliable clinical deployment.

5. Conclusion

The LightBT CNN model achieved a high degree of accuracy, precision, and generalization in brain tumor classification, confirming its effectiveness in distinguishing between glioma, meningioma, pituitary tumors, and healthy brain scans. This study demonstrates the effectiveness of CNN in classifying brain tumors from MRI scans with high accuracy. This interpretability enhances the clinical applicability of deep learning models. However, further optimization of architectures and validation with larger datasets are recommended to enhance efficiency and reduce misclassification. Additionally, the integration of explainable AI tools such as Grad-CAM into medical diagnostics will be essential for building clinician accuracy and ensuring safe adoption of AI-driven diagnostic support systems in healthcare.

6. Limitations of the Study

This study had several limitations that should be acknowledged. First, the dataset size was relatively limited compared to the vast heterogeneity of brain tumor types, which may restrict the generalizability of the findings. Second, while MRI scans were used as the primary imaging modality, differences in image quality, scanner specifications, and acquisition protocols across institutions may have influenced model performance. Third, the study focused only on commonly available CNN architectures without incorporating hybrid or ensemble models,

which could potentially yield higher accuracy. Additionally, the research was primarily computational and did not include real-time clinical validation with radiologists, limiting its immediate clinical applicability. Finally, the models were trained on pre-processed datasets, which may not fully replicate the complexity and noise of real-world clinical MRI images.

7. Future Studies

Future research should aim to address these limitations. Larger, multi-institutional datasets should be used to enhance the robustness and external validity of CNN-based brain tumor diagnosis systems. The integration of multimodal imaging data, such as PET, CT, or advanced MRI sequences, could provide richer diagnostic information and improve classification accuracy. Future studies could also explore the use of ensemble learning, transfer learning with novel architectures, and explainable AI techniques to improve both performance and interpretability. Moreover, clinical validation with radiologists in real-world settings is crucial for translating these models into practice. Finally, the development of lightweight CNN models optimized for deployment on low-resource devices could extend the application of AI-driven diagnosis to regions with limited healthcare infrastructure.

References

[1] S. Kim *et al.*, "Global burden of brain and central nervous system cancer in 185 countries, and projections up to 2050: a population-based systematic analysis of GLOBOCAN 2022," *Journal of Neuro-Oncology*, vol. 175, no. 2, pp. 673-685, 2025/11/01 2025, doi: 10.1007/s11060-025-05164-0.

[2] M. Ait Amou, K. Xia, S. Kamhi, and M. Mouhafid, "A Novel MRI Diagnosis Method for Brain Tumor Classification Based on CNN and Bayesian Optimization," *Healthcare*, vol. 10, no. 3, p. 494, 2022. [Online]. Available: https://www.mdpi.com/2227-9032/10/3/494.

[3] H. Sung *et al.*, "Global Cancer Statistics 2020: GLOBOCAN Estimates of Incidence and Mortality Worldwide for 36 Cancers in 185 Countries," *CA: A Cancer Journal for Clinicians*, vol. 71, no. 3, pp. 209-249, 2021, doi: https://doi.org/10.3322/caac.21660.

[4] D. S. Dizon and A. H. Kamal, "Cancer statistics 2024: All hands on deck," *Cancer Journal for Clinicians*, vol. 74, no. 1, 2024. [Online]. Available: 10.3322/caac.21824.

[5] B. Bonakdarpour and C. Takarabe, "Brain Networks, Clinical Manifestations, and Neuroimaging of Cognitive Disorders: The Role of Computed Tomography (CT), Magnetic Resonance Imaging (MRI), Positron Emission Tomography (PET), and Other Advanced Neuroimaging Tests," *Clinics in Geriatric Medicine*, vol. 39, no. 1, pp. 45-65, 2023, doi: 10.1016/j.cger.2022.07.004.

[6] H. Hu, X. Li, W. Yao, and Z. Yao, "Brain Tumor Diagnose Applying CNN through MRI," in *2021 2nd International Conference on Artificial Intelligence and Computer Engineering (ICAICE)*, 5-7 Nov. 2021 2021, pp. 430-434, doi: 10.1109/ICAICE54393.2021.00090.

[7] W. Ayadi, W. Elhamzi, I. Charfi, and M. Atri, "Deep CNN for Brain Tumor Classification," *Neural Processing Letters*, vol. 53, no. 1, pp. 671-700, 2021/02/01 2021, doi: 10.1007/s11063-020-10398-2.

[8] P. O. Adigun, A. A. Adeniyi, and T. T. Oyekanmi, "Detection and Interpretation of X-Ray Scans for the Presence of Pneumonia Using Convolutional Neural Network," *American Academic Scientific Research Journal for Engineering, Technology, and Sciences*, Original vol. 101, no. 1, pp. 97-108, 2025. [Online]. Available: https://core.ac.uk/download/pdf/640473726.pdf. Yes.

[9] B. A. Mohammed and M. S. Al-Ani, "An efficient approach to diagnose brain tumors through deep CNN," *Mathematical Biosciences and Engineering*, vol. 18, no. 1, pp. 851-867, 2021, doi: 10.3934/mbe.2021045.

[10] A. u. Haq *et al.*, "MCNN: a multi-level CNN model for the classification of brain tumors in IoT-healthcare system," *Journal of Ambient Intelligence and Humanized Computing*, vol. 14, no. 5, pp. 4695-4706, 2023/05/01 2023, doi: 10.1007/s12652-022-04373-z.

[11] C. Sun, "CNN Models Applied in Brain Cancer Diagnosis," in *2021 2nd International Seminar on Artificial Intelligence, Networking and Information Technology (AINIT)*, 15-17 Oct. 2021 2021, pp. 289-293, doi: 10.1109/AINIT54228.2021.00064.

[12] N. Rasool *et al.*, "CNN-TumorNet: leveraging explainability in deep learning for precise brain tumor diagnosis on MRI images," (in eng), *Front Oncol*, vol. 15, p. 1554559, 2025, doi: 10.3389/fonc.2025.1554559.

[13] M. Nickparvar. *Brain Tumor MRI Dataset*, doi: https://doi.org/10.34740/KAGGLE/DSV/2645886.